

⁸H. L. Frish, J. M. Hammersley, and D. J. A. Welch, *Phys. Rev.* **126**, 949 (1962).

⁹S. Kirkpatrick, *Phys. Rev. Lett.* **27**, 1722 (1971), and *Rev. Mod. Phys.* **45**, 574 (1973).

¹⁰T. B. El-Kareh and H. C. Wolf, *Z. Naturforsch.* **22a**, 1242 (1967).

¹¹S. C. Abrahams, J. M. Robertson, and J. G. White, *Acta Crystallogr.* **2**, 233, 238 (1949).

¹²B. J. Last and D. J. Thouless, *Phys. Rev. Lett.* **27**, 1719 (1971).

¹³It is still obvious from Fig. 1 that trap-trap migration and trap-supertrap energy transfer may already play some role between $C_A=0.01$ and 0.05. This would be consistent with the observations ($C_A \leq 0.02$) of K. E. Mauser, H. Port, and H. C. Wolf, *Chem. Phys.* **1**, 74 (1973). However, their statement about "emission from a mixed guest-host exciton band" (at $C_A=0.50$) is inaccurate, in view of the fact that a guest-host band gap does persist (Ref. 5), so that the emission is really

from the bottom of the $C_{10}H_8$ dominated sub-band (the upper $C_{10}D_8$ one being quenched). The mere formation of such a quasicontinuous sub-band resulting in a single emission peak is of course a consequence of percolation (Ref. 5).

¹⁴The oscillator strength of BMN (0-0) seems to be twice that of $C_{10}H_8$ (0-510), according to the absorption experiments of H. M. McConnell and D. D. Tunnicliff, *J. Chem. Phys.* **23**, 917 (1955). Thus our first point ($C_A=0.01$) on Fig. 1 implies that the BMN trapping efficiency is the same as that of $C_{10}H_8$, within a factor of 2 [$C_A=1.21 \times 10^{-2}$; $C_S=(4 \pm 3) \times 10^{-4}$]. For simplicity, we assume it to be $\frac{1}{2}$.

¹⁵Percolation in the triplet state occurs below 10%, showing that the singlet-state percolation is essentially a prompt fluorescence measurement: R. Kopelman, E. M. Monberg, F. W. Ochs, and P. N. Prasad, *J. Chem. Phys.* **62**, 292 (1975).

¹⁶K. Colbow, *Biochim. Biophys. Acta* **314**, 240 (1970).

Effects of Quantum States on the Photocurrent in a "Superlattice"*

R. Tsu, L. L. Chang, G. A. Sai-Halasz, and L. Esaki

IBM Thomas J. Watson Research Center, Yorktown Heights, New York 10598

(Received 13 March 1975)

Photocurrent measurements in GaAs-GaAlAs superlattices grown by molecular-beam epitaxy enable us to observe simultaneously quantum states and associated anomalous conductance. The spectrum in the photocurrent shows a series of peaks of photon energies corresponding to transitions between quantum states in the valence and conduction bands. As a function of applied voltage, the photocurrent exhibits pronounced negative differential conductance when the potential-energy difference between two adjacent wells of the superlattice exceeds the bandwidth of the quantum states.

In this Letter, we report the results of photocurrent measurements in a one-dimensional periodic structure referred to as a semiconductor "superlattice." By examining both the spectral response and the applied-voltage dependence of the photocurrent, we have not only identified quantum states, but also observed their effects in causing a negative differential conductance. Thus, our investigation gives a better exposition of the interrelationship between such quantum states and anomalous transport properties in a superlattice.

It was previously demonstrated that the electron transport properties in well-defined double barriers¹ and periodic structures² were largely governed by quantum states created in these structures. Furthermore, optical-reflectivity measurements³ for a GaAs-AlAs superlattice indicated a shift due to the lowest quantum state of

about 0.1 eV from the absorption edge of GaAs, and absorption spectra⁴ for isolated potential wells showed a series of salient peaks corresponding to bound states and associated excitons. The development of the technique of molecular-beam epitaxy in growing extremely smooth and thin layers of GaAs and $Ga_{1-x}Al_xAs$ has made it possible to observe such quantum states in layered structures.

Superlattice structures of three different configurations have been used in the present experiments: 100 periods of 35-Å-GaAs-35-Å- $Ga_{0.8}Al_{0.2}As$; 80 periods of 50-Å-GaAs-50-Å- $Ga_{0.78}Al_{0.22}As$; and 50 periods of 110-Å-GaAs-110-Å- $Ga_{0.55}Al_{0.45}As$, as labeled by A, B, and C, respectively, in Fig. 1. The total thickness in all cases is of the order of 1 μm which is comparable to the absorption length for the photons involved. The structures were prepared on n -

type, 10^{18}-cm^{-3} GaAs substrates by computer-controlled molecular-beam epitaxy described previously.⁵ Both the periods and compositions are determined from the growth rates which are calibrated by x-ray analyses.⁶ The superlattice region is undoped and an Ohmic contact is made on the bottom of the substrate. A semitransparent Au film $\sim 100 \text{ \AA}$ thick over an area of $0.25 \times 0.025 \text{ cm}^2$ serves as the top electrode. A tungsten source chopped at 1 kHz was usually used in our spectrometer. Normalization for the number of electrons per incident photon is obtained by use of a thermocouple detector for relative light intensity at different photon energies and a Si solar cell calibrated at 9000 \AA for the determination of the absolute flux.

The energy diagram is schematically shown in the upper part of Fig. 1, where quantum states created by the periodic potential are denoted as E_1 and E_2 . These states are essentially discrete for a relatively large separation between wells as is the case in sample C, but broaden into bands in samples A and B as a result of an increase in overlapping of wave functions. Such overlapping results in appreciable conduction as schematically shown in the diagram. The built-in electric field, presented in an exaggerated fashion in the

diagram, arises from the Au-contact Schottky junction, so that the photocurrent flows without any external applied voltage. The field is assumed to be uniform at low-current conditions because of lack of space charge in the superlattice region.

Shown in Fig. 1 is the normalized photocurrent versus photon energy, measured at 5°K under zero bias. It is seen that peaks exist in the spectra for the three different structures. As the superlattice period becomes narrower, the photocurrent increases and the peak positions shift to higher energies with fewer numbers being observed. Particularly, because of the discrete nature of states in sample C, the observed photocurrent is much smaller than those in samples A and B. Calculated energies are indicated by arrows, where E_n is the transition from the n th quantum state of heavy holes in the valence band to that in the conduction band. The combined bandwidth for each transition in samples A and B is also shown, which is mainly determined by electrons. Our experimental results do not indicate a significant increase in photocurrent at the onset of excitation of light holes. The light holes created are able to relax rapidly to the heavy-hole band, and therefore their contributions to transport may be ignored. These results were obtained by use of the Kronig-Penney model based on the configurations of the structures and the following known parameters: well depth $\sim 0.85 \times \Delta E_g$,⁷ $m_e \sim 0.1m_0$ for electrons; and well depth $\sim 0.15\Delta E_g$, $m_h = 0.56m_0$ for holes. The differences of the energy gaps, ΔE_g , are 0.23, 0.25, and 0.55 eV for Al compositions of 20, 22, and 45%, respectively.⁸ As seen in the figure, the general agreement between the experimental result and the theoretical calculation is quite good.

One can estimate the product $\mu\tau$ from the normalized photocurrent in Fig. 1 for zero bias, where μ is the carrier mobility and τ is its lifetime. With neglect of the contribution due to diffusion, the steady-state photocurrent is given by $eAg\mu\tau F$, with e and A being the electronic charge and area, respectively. The generation rate, g , is written as a product $\gamma \times (\text{incident photon flux}) \times (\text{absorption coefficient})$, where γ is about 0.25 in our devices, taking into account reflection losses and absorption due to the thin gold film. The absorption coefficient has been obtained from reflectivity and transmission measurements on superlattice structures having similar configurations.^{3,4} Taking the built-in field F approximated to be $\sim 10^4 \text{ V/cm}$ from the known Schottky-barrier

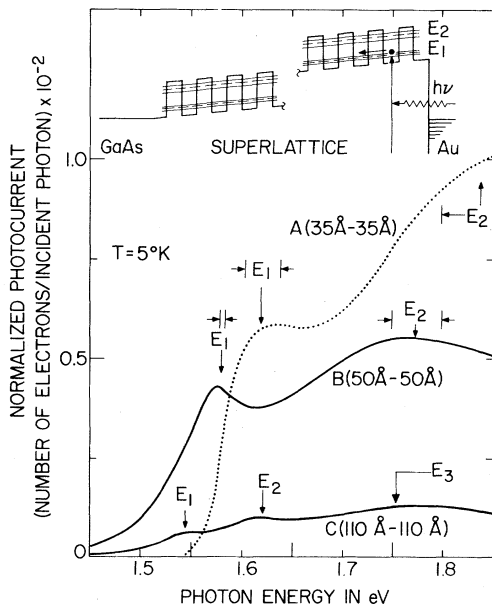


FIG. 1. Normalized photocurrent versus photon energy for three superlattice samples A, B, and C. Calculated energies and bandwidths are indicated. The energy diagram of the Au-contact Schottky barrier is shown in the upper part.

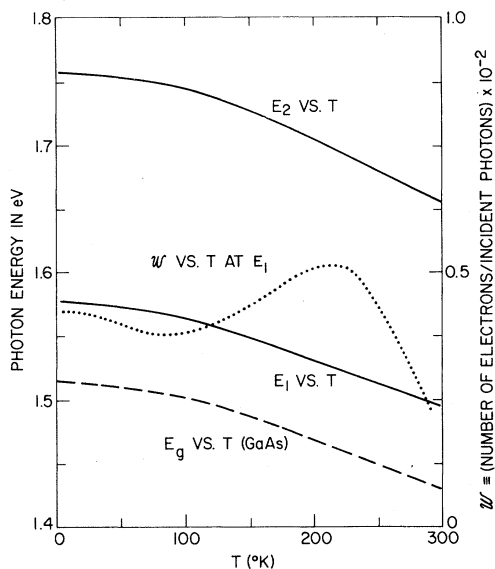


FIG. 2. Temperature dependences of the first and second peaks, E_1 and E_2 , and the normalized E_1 peak height for sample B are shown in solid curves and in a dotted one, respectively, together with that of the GaAs energy gap in a dashed curve.

height,⁹ we find that $\mu\tau$ is 2.5×10^{-10} and 2×10^{-10} cm^2/V at the E_1 peak for samples A and B , respectively. Under the assumption that τ is in the range between 10^{-10} and 10^{-11} sec, μ is estimated to be of the order of $10 \text{ cm}^2/\text{V sec}$, which is consistent with the previous result.²

The temperature dependence of the photocurrent spectra has been measured from 1.8 to 300°K. Shown in Fig. 2 are the peak energies for sample B , where a parallel shift is observed for both E_1 and E_2 with respect to the GaAs energy gap. Such a relationship is expected theoretically, and further establishes the origin of the peaks as due to the transitions between the quantum states in the valence and conduction bands. The dotted curve shows the intensity at the E_1 peak as a function of temperature, showing the existence of the maximum around 200°K.

Figure 3 shows the photocurrent as a function of applied voltage for sample B at three temperatures, 5, 63, and 217°K, and two incident photon energies, E_1 and E_2 . Positive voltage and current here indicate positive voltage applied to the Au electrode and an electron flow toward the substrate. The most striking feature is the presence of a negative differential conductance, as marked by arrows in the figure. In the reverse direction, it is consistently more pronounced with the current peaks occurring near zero bias; while, in

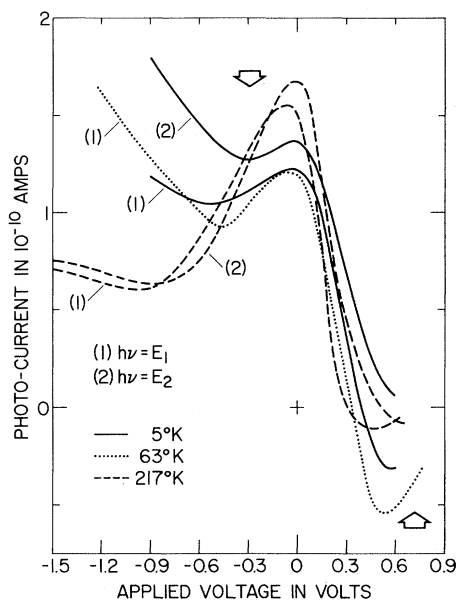


FIG. 3. Photocurrent versus applied voltage for sample B at temperatures 5, 63, and 217°K with incident photon energies E_1 and E_2 (see Fig. 2).

the forward direction, the currents show rather broad minima at voltages around 0.5 V. We have observed similar characteristics for sample A with the threshold voltage of negative conductance occurring at 4.5 V, in the reverse direction. Note that the negative differential conductance is weaker at lower temperatures, possibly because of the increased role of impurity scattering. The dark current at low voltages in the samples is usually an order of magnitude higher than the photocurrent measured, which consists of mainly leakage because of the use of a large, unprotected contact. The dark current increases rapidly at forward bias which prevents us from making measurements at higher voltages. We have noticed considerable instability in the photocurrent which apparently is associated with the onset of the negative conductance.

As it was pointed out previously,² band-type conduction in the superlattice is not expected to be sustained when the potential-energy difference between adjacent wells becomes comparable to the bandwidth. A detailed theory has been developed, based on the phonon-assisted-conduction mechanism.¹⁰ Essentially, at high fields, the electron wave functions become strongly localized within each well region. The decrease of overlapping of the wave functions reduces the current, resulting in a negative differential conductance.

The threshold condition is given approximately by $eFd \sim \Delta E$, where d is the period of the superlattice and ΔE is the width of the band where conduction is taking place. The fact that the photocurrents peak at the same voltage for both E_1 and E_2 in Fig. 3 seems to indicate that electrons generated at the higher band relax to the lower one before transport is effected. The asymmetry of the characteristics arises from the presence of the Schottky barrier which shifts the curve toward positive voltages. The shift, as well as the photocurrent levels at forward voltages, however, are found to be somewhat smaller than those expected from a simple Schottky-barrier model. This may be understood on the basis of the field distortion caused by appreciable electron injection at the GaAs-superlattice interface in the forward-bias condition.¹¹

With this consideration, it is possible to compare the observed threshold with that predicted theoretically. Taking into account the barrier height of Au, we find $eFd \sim 10$ meV compared to $\Delta E_1 \sim 7$ meV as calculated for sample B; and ~ 50 meV compared to $\Delta E_1 \sim 38$ meV for sample A. This consistency establishes the effect of quantum states in causing the observed negative differential conductance, and indicates that electrons generated in the conduction band are mainly responsible for the transport properties.

We are grateful to S. J. Ruffini for his effort in providing the gold films and to C. C. Periu,

M. S. Christie, and L. E. Osterling for their technical assistance.

*Research sponsored in part under contract with the U. S. Army Research Office, Durham, N. C.

¹L. L. Chang, L. Esaki, and R. Tsu, *Appl. Phys. Lett.* **24**, 593 (1974).

²L. Esaki and L. L. Chang, *Phys. Rev. Lett.* **33**, 495 (1974).

³R. Tsu, A. Koma, and L. Esaki, *J. Appl. Phys.* **46**, 842 (1975).

⁴R. Dingle, W. Wiegmann, and C. H. Henry, *Phys. Rev. Lett.* **33**, 827 (1974).

⁵L. L. Chang, L. Esaki, W. E. Howard, and R. Ludeke, *J. Vac. Sci. Technol.* **10**, 11 (1973).

⁶L. L. Chang, L. Esaki, A. Segmüller, and R. Tsu, in *Proceedings of the Twelfth International Conference on the Physics of Semiconductors, Stuttgart, Germany, 1974*, edited by M. H. Pilkuhn (Teubner, Stuttgart, Germany, 1974), p. 688.

⁷The use of $0.85\Delta E_g$ for the determination of the barrier height for electrons is not too critical. Theoretical estimate based on band-structure calculations gives the value around $(0.8 \text{ to } 0.9)\Delta E_g$.

⁸A. Onton, M. R. Lorenz, J. M. Woodall, and R. J. Chicotka, *J. Cryst. Growth* **27**, 166 (1974).

⁹C. A. Mead and W. G. Spitzer, *Phys. Rev.* **134**, A713 (1964).

¹⁰R. Tsu and G. Döhler, *Phys. Rev. B* (to be published).

¹¹See, for example, S. M. Sze, *Physics of Semiconductor Devices* (Wiley-Interscience, New York, 1969), p. 417.

Friction Coefficient of an Adsorbed H Atom on a Metal Surface*

Klaus-Peter Bohnen,[†] Miguel Kiwi,[‡] and Harry Suhl

Department of Physics, University of California, San Diego, La Jolla, California 92037

(Received 23 September 1974)

The friction coefficient η for a hydrogen adatom on a transition-metal surface is calculated in the spirit of a model proposed by Newns. η shows variation over a wide range of values as the adatom approaches the surface. The implications of our results to catalysis are discussed and related to recent work on the subject.

The problem of a physical approach to catalysis has recently received renewed attention; in particular Suhl and co-workers have emphasized that there is a growing body of experimental evidence that catalytic rates show marked anomalies as a result of phase transitions, alloying, or other causes. In addition, very recent results by Krin-

chik² show a remarkably large amplitude modulation of the catalytic rate of the reaction $\text{Ni} + 4\text{CO} \rightarrow \text{Ni}(\text{CO})_4$ as a function of applied magnetic field intensity. In these cases, small systematic changes of the substrate (for example, varying the temperature across a phase transition) do not change the activation energy significantly, while